

Study on Fabrication and Material Properties of Al Doped ZnO Films Prepared by Atmospheric Atomic Layer Deposition

Nghiên cứu chế tạo và tính chất vật liệu của màng mỏng ZnO pha tạp Al
bằng phương pháp lắng đọng từng lớp nguyên tử trong không khí

Thong Quang Trinh^{1*}, Huong Lan Thi Nguyen¹, Phuong Viet Trieu²,
Judith L. MacManus-Driscoll³

¹Hanoi University of Science and Technology, Hanoi, Vietnam

²Vietnam Institute of Standards and Quality, Hanoi, Vietnam

³Department of Materials Science and Metallurgy, University of Cambridge, Cambridge, United Kingdom

*Email: thong.trinhquang@hust.edu.vn

Abstract

This paper presents the study on aluminium-doped zinc oxide (AZO) films prepared by atmospheric atomic layer deposition (AALD) using Diethylzinc (DEZ), $Zn(C_2H_5)_2$, and Trimethylaluminum (TMA), $Al(CH_3)_3$ as precursors. The optimal condition for doping was investigated by changing in DEZ/TMA ratio. The crystal structure of fabricated thin films shows the hexagonal wurtzite structure with the orientation along the c-axis. The influence of heat treatment on the grain size, carrier type and concentration of post-fabricated films deposited on the different substrates which are borosilicate glass and sapphire was also analysed. The Hall measurement to determine the carrier type and resistivity at room temperature to 400 °C was performed. The measurement results show that as-deposited samples behave as alloy-like property with p-type carriers and high resistivity. However, they turned into n-type nature as expected with the increase in carrier concentration and consequently the marked decrease in electrical resistance when annealed at the higher temperatures that are at 500 °C and 900 °C (i.e, 773 and 1173 K). In general, the obtained films with optimized experimental conditions of as- and post-fabrication can be used for thermoelectric applications.

Keywords: AALD, Hall measurement, electrical resistivity, thermoelectric thin films

Tóm tắt

Bài báo trình bày nghiên cứu về màng mỏng ZnO pha tạp Al (AZO) chế tạo bằng phương pháp lắng đọng từng lớp nguyên tử trong môi trường (AALD) sử dụng các tiền chất pha hơi là Diethylzinc (DEZ), $Zn(C_2H_5)_2$ và Trimethylaluminum (TMA), $Al(CH_3)_3$. Điều kiện tối ưu cho quá trình pha tạp đã được khảo sát thông qua thay đổi tỷ lệ tiền chất DEZ/TMA. Cấu trúc tinh thể của màng sau chế tạo có dạng hexagonal wurtzite điển hình với định hướng dọc theo trục tinh thể c. Ảnh hưởng của quá trình xử lý nhiệt lên tính chất dẫn điện của màng trên hai loại đế gồm thủy tinh chịu nhiệt (borosilicate glass) và oxit nhôm (sapphire) cũng đã được phân tích. Phép đo Hall giúp xác định nồng độ hạt tải và điện trở suất ở nhiệt độ phòng. Sự phụ thuộc nhiệt độ của điện trở màng đã được đo trong dải từ nhiệt độ phòng đến 400 °C. Kết quả nhận được cho thấy màng sau chế tạo có cấu trúc giống hợp kim với hạt tải loại p chiếm đa số và điện trở cao. Tuy nhiên, sau khi được nung ủ ở nhiệt độ cao, cụ thể, 500 °C và 900 °C (773 K và 1173 K), tính chất điện của màng đã trở lại là loại n như mong đợi với nồng độ hạt tải tăng và điện trở giảm đáng kể. Có thể nói, màng mỏng AZO chế tạo bằng phương pháp AALD có tương lai hứa hẹn như là vật liệu cho các ứng dụng nhiệt điện sau khi đã được cải thiện điều kiện chế tạo và các biện pháp xử lý sau chế tạo

Từ khóa: AALD, phép đo Hall, điện trở suất, màng mỏng nhiệt điện.

1. Introduction

Providing sustainable energy to the world's population is becoming a major societal problem for the 21st century. Thermoelectric (TE) materials, which are the combination of thermal, electrical, and semiconducting properties, allow converting waste heat into electricity. They are probability to play a more important role in meeting the energy challenge of the future. Recent works on the theory of TE devices

have led to the expectation of enhanced performance by using low dimension materials where the quantum confinement effect occurs. It enables increasing the electronic transport and decreasing the thermal transport for making TE devices more commercially viable.

Transparent conducting intrinsic and doped ZnO thin films have a growing number of interests thanks to their prominent applications in electronic and

optoelectric devices such as gas sensors, thin-film transistors (TFTs) for display technology, light emitting diodes (LEDs), photodetector, solar cells [1], thermoelectric generators (TEGs) and/or thermoelectric coolers (TECs) [2,3]. As an oxide, this n-type material has high electrical resistance leading to low electrical conductivity due to the low carrier concentration that needs to be improved. Accordingly, adding dopants is considered a feasible strategy to increasing the carrier concentration, particularly for TE applications. Hence, aluminium (Al) is one of the common dopants used for this aim. Furthermore, oxide materials have now been becoming a new research trend for TE applications because of their abundance, ease of synthesis, thermal and electrical stability at a wide temperature range in both oxidising and corrosive environments. The recent studies of Al-doped (ZnO:Al or AZO) showed the advanced properties for being the novel TE materials with relatively good Seebeck coefficient [4-6].

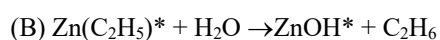
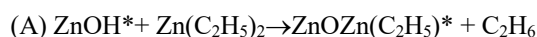
Similar to other materials, pure and doped ZnO thin films can be fabricated by different methods including physical vapor deposition (PVD) like sputtering, pulse laser deposition, chemical vapor deposition (CVD), and wet chemical routes [7]. Nevertheless, the study of alternative ways for getting thin films always motivates the researchers of materials science that is also driving force for us in this work. Atmospheric Atomic Layer Deposition (AALD) is a deposition technique of which the mechanism is similar to the Atomic Layer Deposition (ALD) for growing compound films. This technique relies on a binary sequence of self-limiting surface chemical reactions which typically occur between a gas-phase precursor and a solid surface. Films can be deposited by repeating the binary reaction sequence or a cycle. AALD recently has been developed by the Device Materials Group (DMG), Department of Materials Science and Metallurgy (DMSM), the University of Cambridge [8-10]. By using this technique, the doped ZnO films can be grown employing the alternated cycles of Zn and dopant precursors. It allows the precisely controlling in atomic-scale the concentration, position, and spacing of the dopant in the ZnO lattice. As a result, a typical nanolaminate structure is obtained. The resulting films are usually dense, pinhole-free, and extremely conformal to the underlying substrate. The advanced feature of AALD is that it does not require low pressure, i.e., high vacuum, the capability of large area coating, faster than conventional ALD and compatible with roll-to-roll processing leading to the low-cost products, and more convenient for being applied in industry.

In this paper, a study of AZO films with respect to the ratio of Zn:Al cycles and the heat treatments after film deposition is reported. Phase analysis,

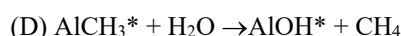
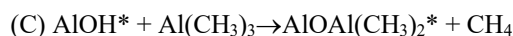
conductivity property demonstrated by carrier type film microstructure, and temperature dependence of sheet resistance were studied to optimize the AALD fabrication of AZO films.

2. Experimental Procedure

Herein, the Al-doped ZnO films are deposited by AALD technique using diethylzinc (DEZ), Zn(C₂H₅)₂ vapor as the Zn precursor, trimethylaluminum (TMA), Al(CH₃)₃ vapor as the Al precursor and water vapor as oxidizer. In this case, ZnO atomic layer is performed using alternating DEZ (precursor 1) and H₂O exposures in the A and B reaction, respectively, as follows



Similarly, Al₂O₃ atomic layer is performed using alternating TMA (precursor 2) and H₂O exposures



where the asterisks represent the surface species. By repeating these reactions in an ABCD sequences via scanning procedure, AZO films can be deposited with atomic layer control as illustrated in Fig. 1a and 1b. The total flow rate for both precursors was kept constant at 25 ml.min⁻¹. Consequently, the flow rate ratio of each precursor lines was individually adjusted as 15/10, 17/8, 19/6, 21/4, and 23/2 ml.min⁻¹ while this parameter for the oxidizer line is 2050 ml.min⁻¹. Argon (Ar) gas was passed through the bubblers containing the different precursors at gas flow rates of 50 ml.min⁻¹. The total time for deposition was set 15 minutes. After growth, the gases were switched off and the substrates left to cool naturally in the open atmosphere. The AALD system used for this study is shown in Fig. 1c. Two series of ZnO/Al₂O₃ films with different ZnO/Al₂O₃ cycle ratios were grown. Films were deposited on glass (sodalime and borosilicate) and sapphire substrates at 300 °C (573 K). The substrates were scanned under the head at a rate of 50 mm.s⁻¹. A set of samples deposited on soda lime glass was subsequently annealed at 500 °C (773 K). The other set of samples deposited on sapphire was annealed at 900 °C (1173 K). The annealing time was kept for 5 hours in nitrogen environment to prevent the chemical diffusion process during the growth of the crystalline phase.

X-ray diffraction (Cu-Kα, Siemen D5005 Brucker, (λ = 1.54056 Å) was employed to identify the crystal structure and phase of the samples. SEM Hitachi S-4800 system was used to examine the grain size and morphology.

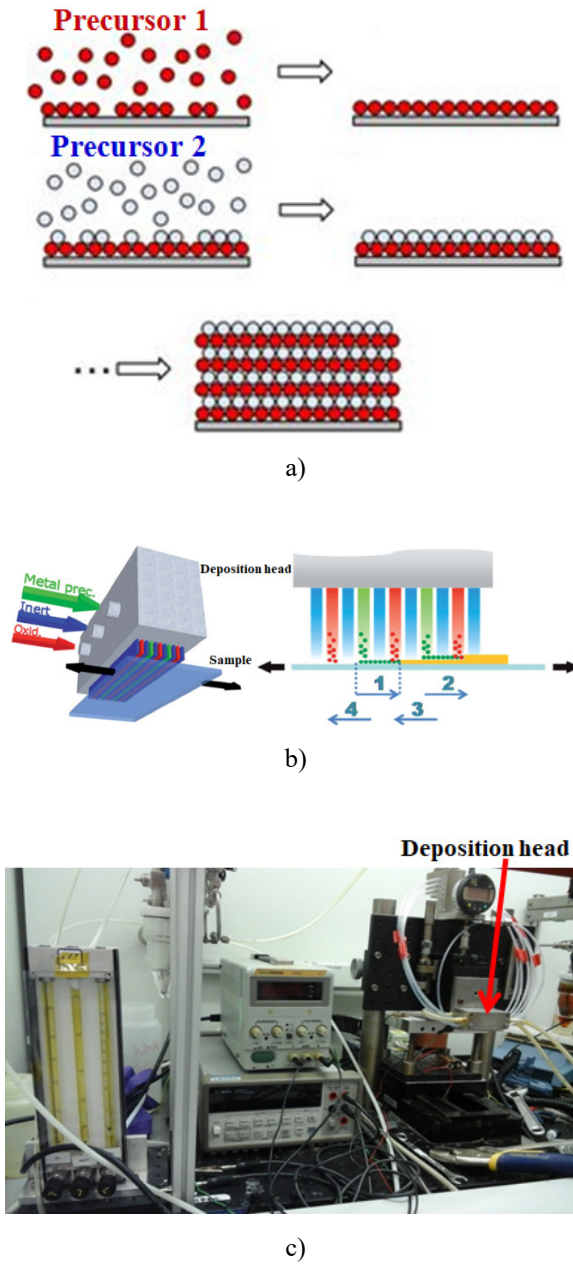


Fig. 1. Film atomic layer deposition, a) mechanism of film formation, b) scanning mechanism for film deposition, c) AALD system

The Hall Effect measurement is based on the Van der Paw method. A magnetic field of 1 T was applied for the measurements. The carrier concentration was determined from the Hall voltage, current used, magnetic field strength and charge type. From the calculated resistivity and carrier concentration, the mobility for each sample was calculated. The resistivity was calculated from the sheet resistance obtained and the measured film thickness, which is determined using the stylus profiler.

In this work, we have designed and fabricated an

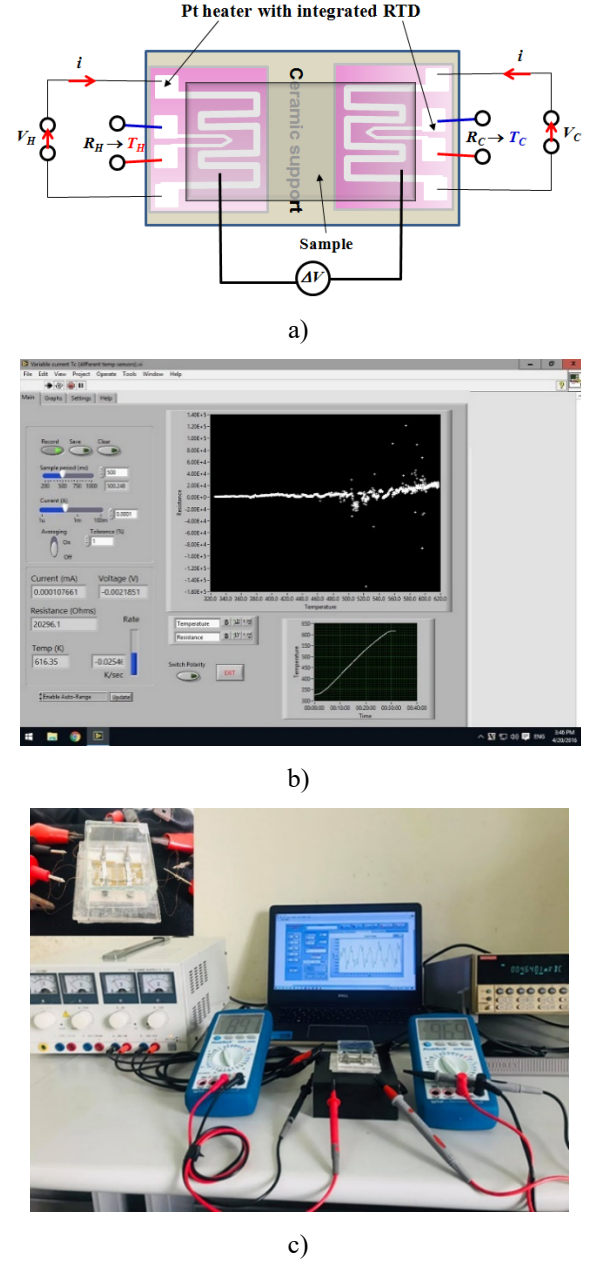


Fig. 2. a) Structure and arrangement of integrated devices and measured sample, b) Labview interface of measurement program, c) entire of measurement setup for temperature-dependent sheet resistance (the inset is zoom-in image of a measured sample)

automated apparatus for measuring the sheet resistances of ZnO/Al₂O₃ films in the planar geometry over a range between room temperature to 400 °C that is from 300 to 673 K (Fig. 2a). The principal structure of our measurement setup is shown in Fig. 2a. It consists of two heat sinks enabling the temperature difference that can be measured by using the appropriate devices as well as the voltage difference between two ends of the material. Herein, we propose a device including a micro-heater and an integrated resistance temperature detector so-called Pt-100 RTD

instead of the traditional thermocouple. The measurement principle of RTD sensor is based on the change in resistance (R_H , R_C) of platinum that is proportional to temperature (T_H , T_C). It should be noted that Pt is a metal having low resistivity and good thermal response at relatively low voltages. In addition, its resistivity also exhibits a positive and highly linear dependence on temperature. Besides, Pt shows excellent long-term stability, it is chemically inert and has the well-established manufacturing processes. By implementing an appropriate design, the Pt thin film could be able to act simultaneously as both a heater and a sensor. The measurement data were acquired continuously by a LABview programme as illustrated in Fig. 2b. Lastly, Fig. 2c is the image of the measurement setup used for the investigation of temperature-dependent sheet resistance of samples fabricated in this study.

3. Results and Discussion

The average thickness of all obtained films was measured around 300 nm. The crystal structure of films was investigated for as-deposited samples and those annealed at 500 °C and 900 °C. The annealing temperature of 500 °C was used for the first heat treatment of the sample set deposited on the glass substrate relying on our investigations to optimize the regime for crystalline formation. For the as-grown samples before heat treatment, the XRD result shows the degradation of the film crystalline when the Al content is increased (Fig. 3a). As ratio of 15/10 and 17/8, the samples are totally poor in film crystalline and no $ZnAl_2O_4$ phase is detected. It seems they are non-crystalline suggesting just the amorphous-like insulating characterization (such as Al_2O_3) presented in the films. As the ratio of 19/6, 21/4, and 23/2 the diffraction trace of the (002) plane is also evidently weak. It should be noted that only the (100) and (101) peaks of the hexagonal phase ZnO appear and no crystalline Al_2O_3 or $ZnAl_2O_4$ peaks are detectable in the X-ray diffraction patterns. After being annealed at 500 °C, we can see the XRD spectra of the samples deposited on the glass substrate which indicates more clearly the crystal structure (Fig. 3b).

There can be seen a little bit of change in phase for samples with a ratio of 15/10 and 17/8. Maybe a two-phase mixture of ZnO hexagonal and Al_2O_3 rhombohedral in structure occurred. For the samples with ratio of 23/2, 21/4, and 19/6, it begins demonstrating the typical crystal structure of ZnO. This result indicates that partial crystallization was promoted due to heat treatment. To consider more clearly the influence of the heat treatment process on crystal structure, the sample set deposited on sapphire substrates was annealed at 900 °C (Fig. 3c). It can be observed that further heating at higher temperature produced a well-crystallized material, even for samples having ratio of 15/10 and 17/8. The obtained results in our study are similar to those ones attained

by previous reports for AZO films deposited by ALD method [11]

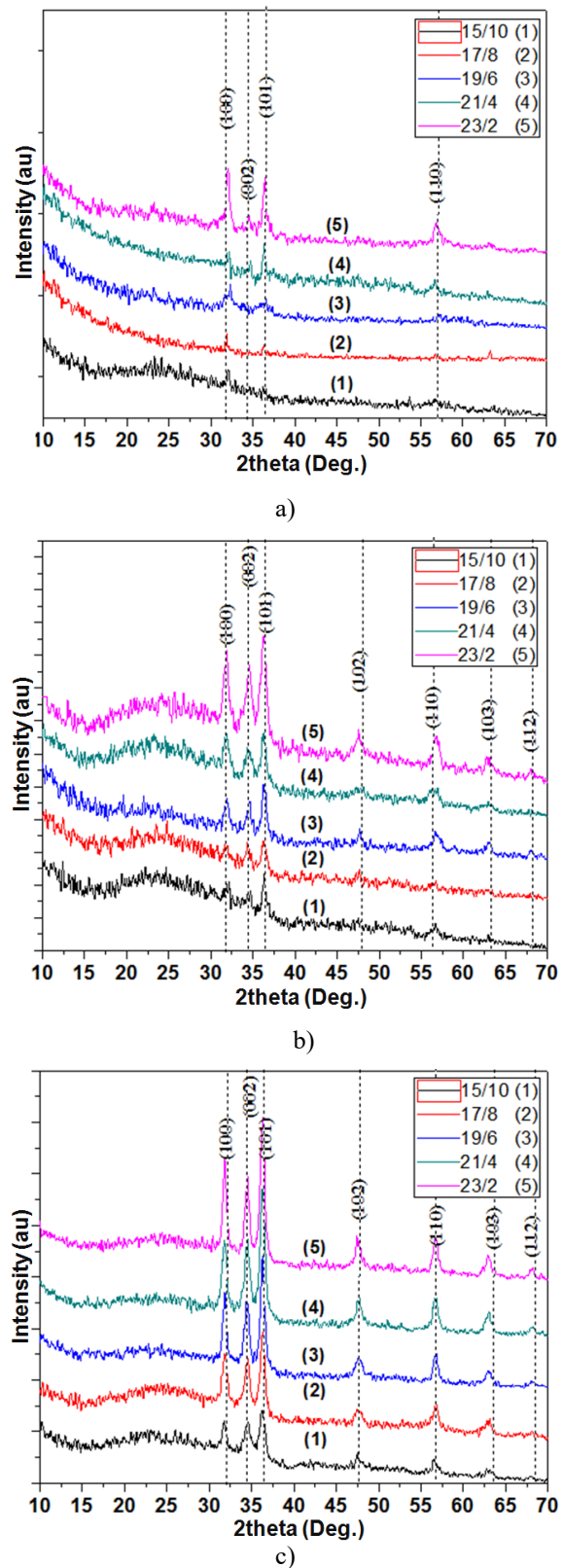
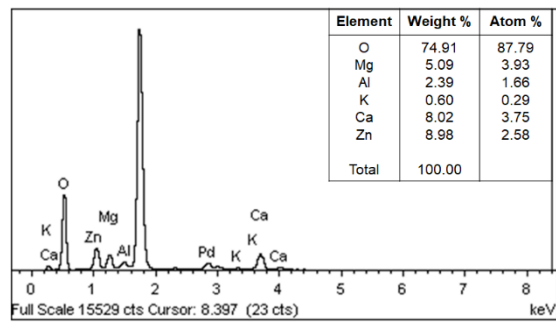
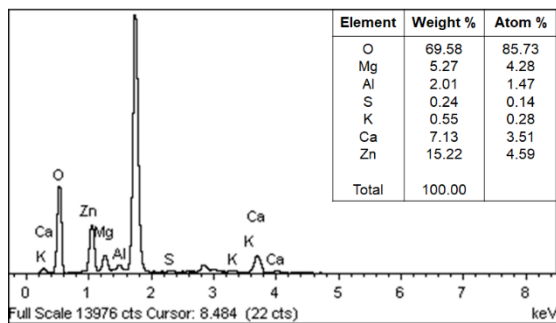


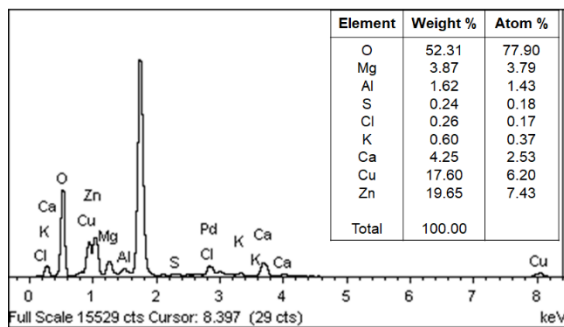
Fig. 3. XRD profiles of AZO films as-deposited (a), annealed at 500 °C (b), and annealed at 900 °C (c)



a)



b)

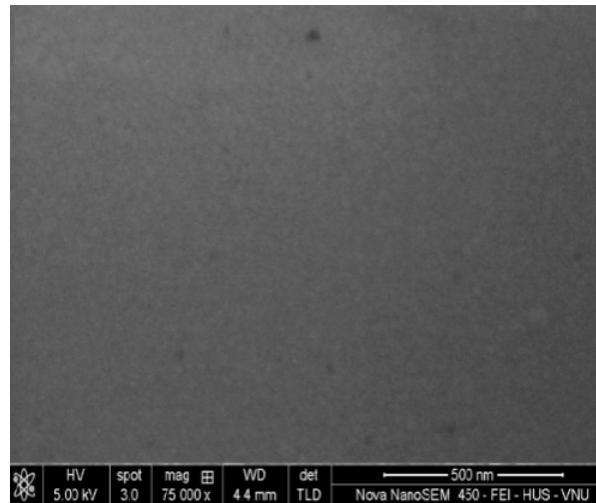


c)

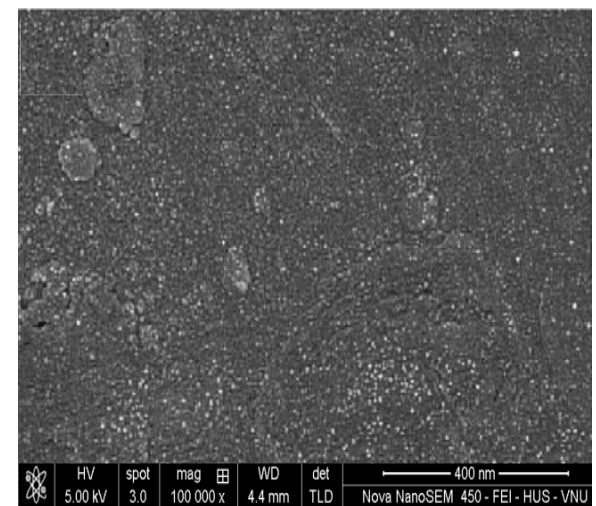
Fig. 4. EDX spectrum of films on sodalime glass slides with ratio of DEZ/TMA as 19/6 (a), 21/4 (b), and 23/2 (c)

The obvious existence of the peak corresponding to (002) plane shows the c-axis preferential orientation of the films. It is very important because the films oriented with the c-axis normal to the substrate would show a lower sheet resistance than those with randomly oriented.

Fig. 4 shows the typical EDX spectra of as-deposited films on the glass substrates with the ratios 19/6, 21/4, and 23/2 which were selected to compare the chemical composition of samples after being fabricated. The analysis results revealed that only the films with a ratio of 21/4 have an Al content of about 2 wt.%. This concentration of Al in ZnO is well-known the best for the TE applications [4-6]. Thus, the



a)



b)

Fig. 5. SEM images of as-deposited films with ratio of 15/10 (a) and 21/4 (b)

samples with the ratio of 21/4 were chosen in the next investigations of morphology and electrical properties.

Fig. 5 selectively displays the surface SEM images of typical samples having the ratio 15/10 and 21/4 prepared in our study. The SEM image shown in Fig. 5a is corresponding to as-deposited films with a ratio of 15/10. It can be seen that the films' surface looked the homogenous structure. Fig. 5b is for the sample with ratio of 21/4 we can observe more clearly the grain structure. It means that the crystal phase was really formed. Two images of films with ratio 21/4 are displayed in Fig. 6 for two cases of the heat treatment. Obviously, when annealed at temperature of 500 °C, the crystalline grains have significantly increased size as shown in Fig. 6a. They continue to grow up with

bigger size at annealing temperature of 900 °C (Fig. 6b) for the samples deposited on sapphire substrates. It can be said that the heat treatment process changed the crystalline grains and made their distribution more uniform provided by the visible fact over the films.

As a result of the EDX analysis and SEM images shown in Fig. 4, 5, and 6, the samples with the ratio of 21/4 were used for investigating the electrical property of AZO films. The results of the Hall-effect measurements are summarized in Table 1. Incredibly, the as-deposited samples and those annealed at 500 °C present the p-type conductivity with the hole concentration of about 10^{15} cm^{-3} and 10^{13} cm^{-3} , respectively. It is opposite to the native electrical property of ZnO and Al-doped ZnO known as n-type one. The reason may come from the way to grow the films by AALD. The water vapor as an oxidizer easily is evaporated at the deposition temperature of 300 °C in the atmosphere. It results in the lack of the elements which are oxygen and hydrogen as deep and swallow donors to contribute to the n-type conductivity [12]. Instead, this process can lower the formation energy of some acceptor defect, such as zinc vacancy and thus accounts for the p-type conductivity.

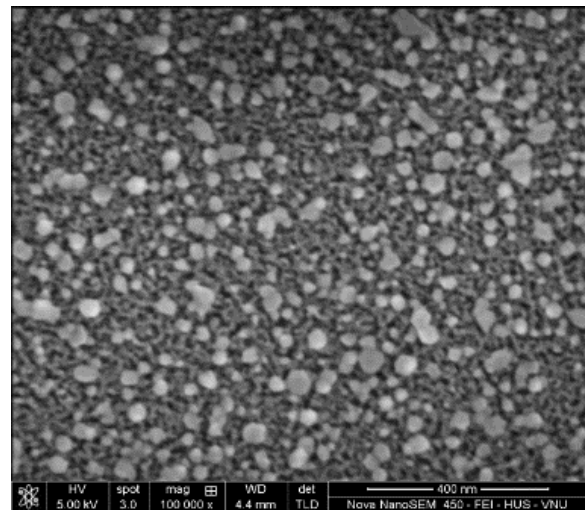
The films annealed at 500 °C show a decrease of p-type signal with a lower hole concentration of 10^{14} cm^{-3} , indicating a carrier-type transition around this temperature demonstrated by the presence of n-type carriers in Hall measurement files. Only being annealed at a relatively high temperature at 900 °C the films represent the n-type conductivity with an electron concentration around 10^{16} cm^{-3} . The inversion to n-type conductivity can be understood as the compensation effect by the ionized oxygen vacancy donor, which is ready to form at high temperatures. The high values of mobility for the as-deposited films and those annealed at 500 °C suggested that the behavior of obtained compounds in these conditions is not oxide but alloy-like. This behavior of the films is not suitable for TE applications. Therefore, annealing at a higher temperature is needed to get the desired films as oxides.

Interestingly, the resistivity of the film deposited on sapphire was measured to be 19.3 Ω.cm. This is substantially lower than the resistivity of all the AZO films grown on glass, which had resistivity values of 178.5 Ω.cm and 39.4 Ω.cm. It demonstrates that the nucleation direction of crystalline grains during the AALD cycles can be influenced by using the appropriate substrate.

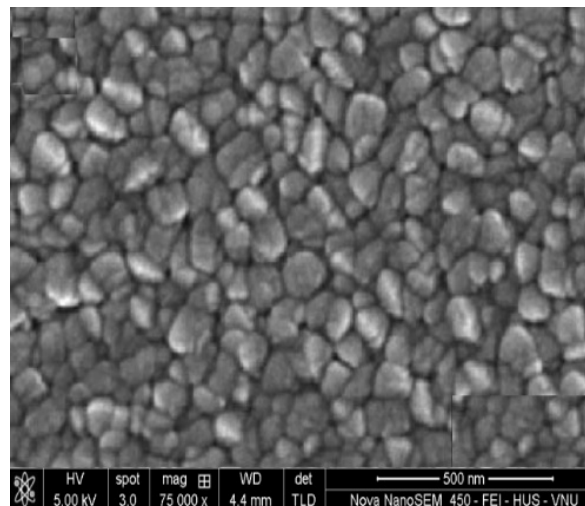
For the aiming at TE applications of fabricated films, the temperature-dependent sheet resistance of films with the ratio of 21/4 under different heat treatments was investigated. Fig. 7 shows the variation of sheet resistance of AZO films for the measured range of room temperature (300 K) to 400 °C (700 K).

Table 1. Electrical properties of AZO thin films at different temperatures

Temperature (°C)	300	500	900
Resistivity (Ω.cm)	178.5	39.4	19.3
Hall mobility (cm ² /V.s)	2218	1035	85
Carrier concentration (cm ⁻³)	1.39 x 10 ¹⁵	1.45 x 10 ¹³	2.71 x 10 ¹⁶
Carrier type	p	p & n	n



a)



b)

Fig. 6. SEM images of films with ratio of 21/4 annealed at 500 °C (a) and 900 °C (b)

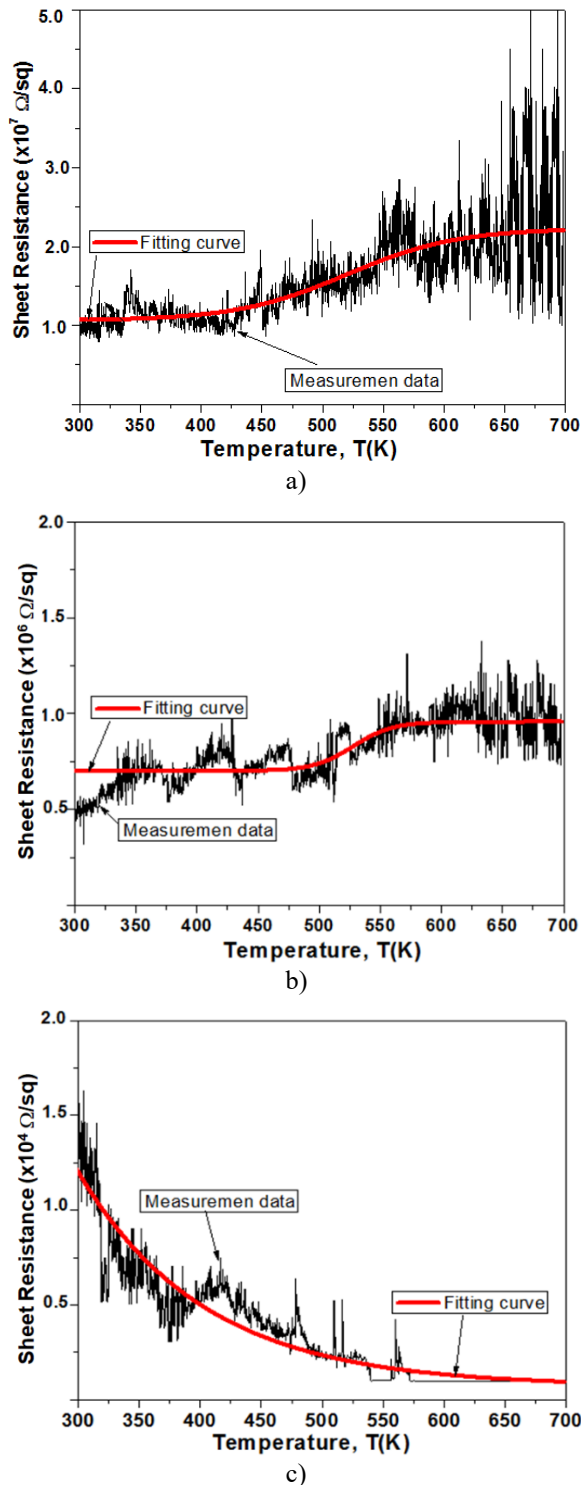


Fig. 7. Temperature-dependent sheet resistance of as-deposited films (a), films annealed at 500 °C (b), and films annealed at 900 °C (c)

For the as-deposited samples the sheet resistance increases a little bit as temperature increases (Fig. 7a). This result agrees with the Hall measurement one confirming that the compound of these films is as likely as an alloy, not a semiconductor. The value of sheet resistance varies in a range between $1 \times 10^7 \Omega/\text{sq}$ at room temperature to $2 \times 10^7 \Omega/\text{sq}$ at 400 °C (or

673 K). For the samples annealed at 500 °C, this tendency was changed as shown in Fig. 7b. The values of sheet resistance in the measured temperature range were one order smaller than those for as-deposited films. Namely, there is only a small increase in the range of 450 K and 550 K implying that AZO films incline to be characteristic of semiconductors. The smallest and highest values are $6 \times 10^5 \Omega/\text{sq}$ at room temperature to $8 \times 10^5 \Omega/\text{sq}$ at 400°C. For the samples annealed at 900 °C, we can see that the films' resistance decreases as temperature increases confirming the property of an n-type semiconductor (Fig. 7c) as the result of Hall measurement shown in Table 1. The sheet resistance of these films was remarkably improved, and its absolute values decrease three to four orders compared to the as-deposited ones that are $1.25 \times 10^4 \Omega/\text{sq}$ at room temperature and $1.9 \times 10^3 \Omega/\text{sq}$ at 400°C. The improvement of sheet resistance of annealed samples can be understood by the increase in grain size, carrier type and concentration indicated by Hall measurements and SEM investigations. However, the only remained issue is that the values of film resistance were still a little bit high that may be related to the low carrier concentrations as shown in Hall measurement results. This may be a disadvantage of the AALD system for the film deposition used in this study that needs to improve in the next research works.

4. Conclusion

AZO films were prepared by atmospheric atomic layer deposition (AALD) of AZO films using DEZ, TMA, and water vapor. A deposition temperature of 300°C was selected for growing the AZO films on borosilicate glass and sapphire substrates. The composition of the films was controlled by adjusting the DEZ/TMA ratios of 15/10, 17/8, 19/6, 21/4, and 23/2 that is ZnO ALD and Al_2O_3 ALD reaction cycles in the ejected sequence. The XRD analysis showed different characterizations of the as-deposited films depending on the DEZ/TMA ratios. The amorphous-like structure is for films with more Al content corresponding to the ratio of 15/10 and 17/8. In general, the crystal structure was improved by annealing at 500 °C and 900 °C in a nitrogen environment. The EDX study determined that the DEZ/TMA ratio of 21/4 is best appropriate to grow the AZO films for TE applications. The SEM images also well confirmed those results. The Hall effect measurements indicated the as-deposited films have p-type conductivity. The origin of p-type behavior can be ascribed to the formation of zinc vacancy and some possible complex acceptor centers. The cause may be due to the evaporation of water vapor as an oxidizer at the deposition temperature of 300 °C in the atmosphere. Understanding these intrinsic acceptor states will help elucidate the extrinsic as well as intrinsic p-type of AZO films. In addition, the carrier mobility which was calculated by Hall effect

measurements revealed that the as-deposited films are alloy-like behavior. Both these behaviors can also be tuned by the heat treatment at 500 °C. The temperature-dependent sheet resistance demonstrated the n-type conductivity and semiconductor's behavior when the films were annealed at 900 °C. Enhanced resistance was observed in annealed films deposited on sapphire (0001) substrates due to the increase in grain size and carrier concentration as shown by SEM images and Hall measurement.

Acknowledgments

This work has been financially supported by Vietnam's National Foundation for Science and Technology Development (NAFOSTED), Ministry of Science and Technology (MOST), under the Grant number 103.02-2017.304.

References

- [1] Sumit Vyas, A short review on properties and applications of zinc oxide based thin films and devices, Johnson Matthey Technol. Rev., 64 (2), pp. 202–218 2020
<https://doi.org/10.1595/205651320X15694993568524>.
- [2] Xuxuan Chen, Zhifang Zhou, Yuan-Hua Lin, Cewen Nan, Thermoelectric thin films: Promising strategies and related mechanism on boosting energy conversion performance, Journal of Materiomics, Vol. 6, pp. 494-512, 2020
<https://doi.org/10.1016/j.jmat.2020.02.008>.
- [3] Chuanle Zhou, Amirhossein Ghods, Kelcy L. Yungans, Vishal G. Saravade, Paresh V. Patel, Xiaodong Jiang, Bahadır Kucukgok, Na Lu, Ian Ferguson, ZnO for solar cell and thermoelectric applications, Proc. in Oxide-based Materials and Devices VIII, SPIE OPTO, San Francisco, California, United States, 2017, Vol. 10105, 101051K
<https://doi.org/10.1117/12.2262772>.
- [4] P. Mele, S. Saini, H. Honda, K. Matsumoto, K. Miyazaki, Effect of substrate on thermoelectric properties of Al-doped ZnO thin films, Appl. Phys. Lett. 102, p. 253903, 2013
<https://doi.org/10.1063/1.4812401-1-4>
- [5] S. Saini, P. Mele, H. Honda K. Matsumoto K. Miyazaki, and A. Ichinose, Thermoelectric properties of Al-doped ZnO thin films, J. of Elect. Mater., 43(6), pp. 2145-2150, 2014
<https://doi.org/10.1007/s11664-014-2992-x>.
- [6] Joana Loureiro, Nuno Neves, Raquel Barros, Tiago Mateus, Rafael Santos, Sergej Filonovich, Sebastian Reparaz, Clivia M. Sotomayor-Torres, Frederic Wyczisk, Laurent Divay, Rodrigo Martinsa and Isabel Ferreira, Transparent aluminum zinc oxide thin films with enhanced thermoelectric properties, J. of Mater. Chem. A, The Royal Society of Chemistry, iss.2, pp. 6649-6655, 2014
<https://doi.org/10.1039/C3TA15052F>.
- [7] Michał A. Borysiewicz, ZnO as a functional material, a review, Crystals, 9(10), p. 505, 2019
<https://doi.org/10.3390/cryst9100505>.
- [8] David Munoz-Rojas and Judith MacManus-Driscoll, Spatial atmospheric atomic layer deposition: a new laboratory and industrial tool for low-cost photovoltaics, Mater. Horiz., The Royal Society of Chemistry, Vol .1, pp. 314-320, 2014
<https://doi.org/10.1039/C3MH00136A>
- [9] Robert L. Z. Hoyer, David Muñoz-Rojas, Shelby F. Nelson, Andrea Illiberi, Paul Poodt, Fred Roozeboom, and Judith L. MacManus-Driscoll, Research update: Atmospheric pressure spatial atomic layer deposition of ZnO thin films: Reactors, doping, and devices, J. Appl. Phys. Lett., APL Materials 3, p. 040701, 2015
<https://doi.org/10.1063/1.4916525>.
- [10] D. Muñoz-Rojas, M. Jordan, C. Yeoh, A. T. Marin, A. Kursumovic, L. A. Dunlop, D. C. Iza, A. Chen, H. Wang, and J. L. MacManus Driscoll, Growth of $\sim 5 \text{ cm}^2\text{V}^{-1}\text{s}^{-1}$ mobility, p-type copper(I) oxide (Cu₂O) films by fast atmospheric atomic layer deposition (AALD) at 225°C and below, AIP Advances 2, pp. 042179, 2012
<https://doi.org/10.1063/1.4771681>.
- [11] Hou, Q., Meng, F. & Sun, J. Electrical and optical properties of Al-doped ZnO and ZnAl₂O₄ films prepared by atomic layer deposition, Nanoscale Res Lett Vol. 8, pp. 144, 2013
<https://doi.org/10.1186/1556-276X-8-144>.
- [12] S. J. Jokela and M. D. McCluskey, Structure and stability of O-H donors in ZnO from high-pressure and infrared spectroscopy, Phys. Rev. B, 72, pp.113201, 2005
<https://doi.org/10.1103/PhysRevLett.72.113201>.